Temperature dependence of the nonlocal voltage in an Fe/GaAs electrical spin-injection device

G. Salis,* A. Fuhrer, R. R. Schlittler, L. Gross, and S. F. Alvarado
IBM Research-Zurich, Säumerstrasse 4, 8803 Rüschlikon, Switzerland
(Received 23 March 2010; revised manuscript received 23 April 2010; published 28 May 2010)

The nonlocal spin resistance is measured as a function of temperature in a Fe/GaAs spin-injection device. For nonannealed samples that show minority-spin injection, the spin resistance is observed up to room temperature and decays exponentially with temperature at a rate of 0.018 K^{-1}. Postgrowth annealing at 440 K increases the spin signal at low temperatures but the decay rate also increases to 0.030 K^{-1}. From measurements of the diffusion constant and the spin lifetime in the GaAs channel, we conclude that sample annealing modifies the temperature dependence of the spin-transfer efficiency at injection and detection contacts. Surprisingly, the spin-transfer efficiency increases in samples that exhibit minority-spin injection.

DOI: 10.1103/PhysRevB.81.205323 PACS number(s): 72.25.−b, 73.40.Gk, 85.75.−d

The efficient injection of spin-polarized electrons from a ferromagnetic source into a semiconducting channel is a fundamental ingredient of spin-based electronic device concepts. The injected spin polarization can be detected by analyzing the degree of circular polarization of photons that are emitted from the semiconductor after recombination of the injected electrons with resident holes.[1–5] In all-electrical devices, the concept of nonlocal spin detection[6–12] has been used to convert spin polarization into a nonlocal voltage ΔU_{nl} that is measured at a ferromagnetic detection contact to which the injected electron spins diffuse. This voltage depends not only on how efficient spins are injected and detected but also on the loss of spin polarization during the diffusive spin transport in the semiconductor. For electrical spin injection into GaAs, a rapid decay of ΔU_{nl} with temperature has been reported,[8,9] in contrast to the measured circular polarization of electroluminescence that remains observable up to room temperature[4] and is strongly influenced by the interplay of spin lifetime and radiative-recombination time.[13] For Fe on GaAs(001), the sign and magnitude of the measured spin injection depend delicately on the growth temperature of the Fe layer as well as on a postgrowth annealing treatment, where a reversal from minority- to majority-spin injection has been observed.[14] Postgrowth annealing also has a strong influence on the magnetic properties of ferromagnetic thin films on III-V compounds.[15,16]

Here we report a considerable change in the temperature dependence of the spin-transfer efficiency across the ferromagnet/semiconductor interface that occurs after annealing Fe/GaAs samples at moderate temperature. We investigate the nonlocal spin resistance $\Delta\rho_{\mathrm{nl}}=\partial\Delta U_{\mathrm{nl}}/\partial I$ as a function of temperature T up to 300 K (I is the current across the spin-injection contact). Between 5 and 200 K, we find an exponential decay of $\Delta\rho_{\mathrm{nl}}$ with T at a rate that depends strongly on the annealing conditions. After annealing the sample at 440 K, $\Delta\rho_{\mathrm{nl}}(T)$ decays considerably faster as compared to nominally nonannealed samples that have seen a maximum temperature of 390 K. In order to understand this T dependence, we write $\Delta\rho_{\mathrm{nl}}\propto\eta_i\eta_d S$, where the spin-injection efficiency η_i specifies the spin polarization of an electron that has just tunneled from the Fe-injection contact into the GaAs channel, the spin-detection efficiency η_d describes the relation between the spin polarization below the detection contact and ΔU_{nl}, and the spin decay S is a factor that accounts for the loss of spin polarization during the diffusive transport in the semiconductor between injection and detection contacts. By measuring the spin lifetime τ_s and the diffusion constant D in the channel, we determine $S(T)$. Since $S(T)$ does not change after sample annealing, the strong modification of $\Delta\rho_{\mathrm{nl}}(T)$ must arise from a change in $\eta_i(T)$ and/or $\eta_d(T)$. For annealed samples, $\eta_i\eta_d$ is almost independent on T, whereas for those nonannealed samples that show minority-spin injection, $\eta_i\eta_d$ rises with T between 30 and 140 K. This unexpected result is discussed in terms of interface-related mechanisms that favor minority-spin transfer across the interface as an increase in T is modifying the energy of the relevant electrons.

The samples under investigation consist of an n-doped GaAs spin-transport layer and Fe contacts for spin injection and detection. The spin-transport channel is formed by a 1000-nm-thick n-doped GaAs epilayer with Si doping concentration of 5×10^{16} cm^{-3}, except in the uppermost 30 nm, where the doping concentration was gradually increased to 5×10^{18} cm^{-3} as described in Ref. 17. After thermal desorption of a protective As layer in ultrahigh vacuum, 5 nm of Fe and 2 nm of Au were evaporated through a nanostencil mask[18] with a pattern of four 56-μm-long bars, see Fig. 1(a). These bars are electrically contacted by 100-nm-thick TiAu that is insulated from GaAs by a 100-nm-thick Al_2O_3 layer. The middle bars (2 and 3) serving as spin injection and detection contacts are 1 and 3 μm wide and separated by a gap of $a=2.4$ μm. Between contacts 1 and 2, a bias U_0 is applied. For positive U_0, spin-polarized electrons are injected at contact 2 into the spin-transport channel and drift toward contact 1. For negative U_0, electrons drift from contact 1 to contact 2 and spin polarization accumulates below contact 2 because of spin filtering.[8] In both cases, spin polarization diffuses toward contact 3, where a potential U_{nl} with respect to contact 4 is measured. When switching the alignment of the magnetizations of the injection and detection contacts from antiparallel to parallel with an external magnetic field B, a change in U_{nl} is observed by an amount ΔU_{nl} that is proportional to the average spin polarization below the detection contact. From measurements using a lock-in amplifier, we obtain $\rho_{\mathrm{nl}}=\partial U_{\mathrm{nl}}/\partial I$, from which U_{nl} and ΔU_{nl} are determined by integration over I. The voltage drop U_{c} across the Schottky barrier of contact 2 is measured as a potential difference between contacts 3 and 2.

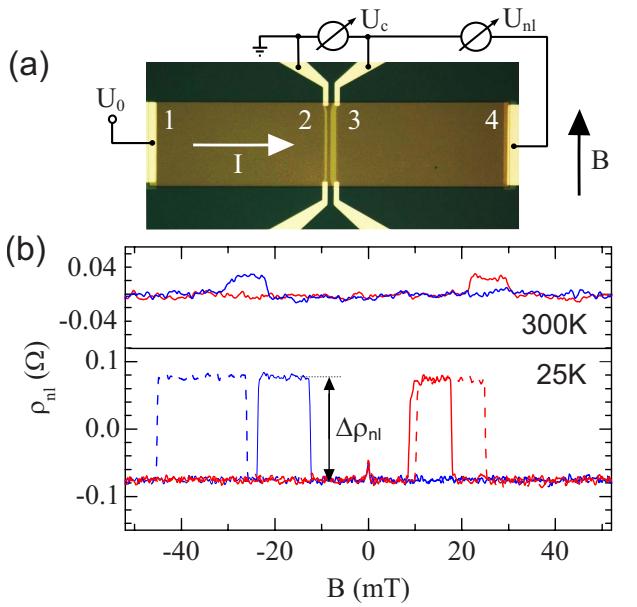

FIG. 1. (Color online) (a) Microscope image of the device consisting of four Fe bars, with the two inner bars serving as injection (2) and detection (3) contacts, whereas the outer bars (1 and 4) are used as reference contacts for spin injection and for measurement of U_{nl}. (b) Measured nonlocal resistance ρ_{nl} for a nonannealed sample at $U_c=-100$ mV. At 25 K, the magnetization reversal (steps $\Delta\rho_{nl}$) occurs at stochastic switching fields, and single up (red) and down (blue) sweeps are shown. At higher T, repeatable switching fields are observed. Data at 300 K are averaged over ten sweeps. A background was subtracted that is linear in B.

From data of ρ_{nl} versus B we determine $\Delta\rho_{nl}$, see Fig. 1(b). For nonannealed samples, $\Delta\rho_{nl}$ decreases by a factor of 80 between 5 and 300 K. The values for ΔU_{nl} versus U_c are shown in Fig. 2 for T between 5 and 125 K. We find a nonmonotonic dependence of ΔU_{nl} on U_c. It is helpful to consider that ΔU_{nl} is proportional to the product of I and the spin-injection efficiency, $\eta_i(U_c)$, such that $\eta_i \propto \Delta U_{nl}/I$. We

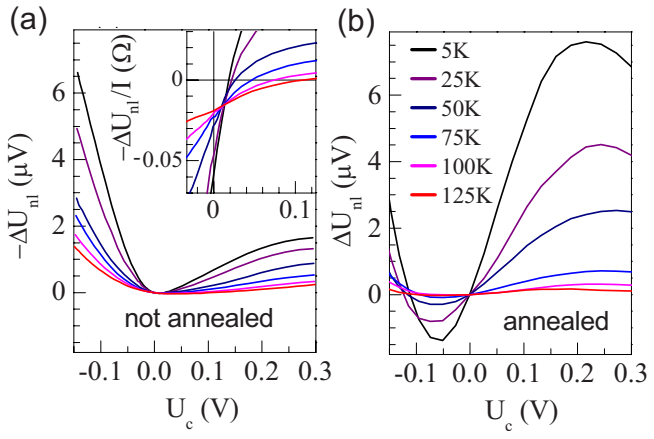

FIG. 2. (Color online) Bias dependence of ΔU_{nl} vs U_c, for different T (a) before and (b) after annealing. In nonannealed samples, a sign reversal of ΔU_{nl} for positive U_c (spin injection) is observed whose position shifts to higher U_c as T is increased, see inset of (a) where $-\Delta U_{nl}/I$ is plotted. Annealed samples exhibit a sign reversal of ΔU_{nl} for negative U_c.

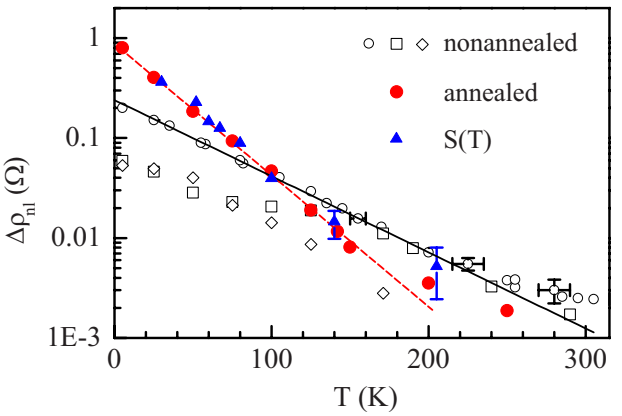

FIG. 3. (Color online) Temperature dependence of $\Delta\rho_{nl}$ of the samples before and after annealing. For the nonannealed samples, data for $U_c=-100$ (circles), 0 (squares), and 200 mV (diamonds) are shown. For the annealed sample, $U_c=0$ mV. The solid and dashed lines are exponential decays with rates of 0.018 and 0.030 K^{-1} for the nonannealed and annealed samples, respectively. Filled (blue) triangles represent $S(T)$, i.e., the expected signal as calculated using D from Hall measurements and τ_s from one-parameter Hanle fits assuming temperature-independent spin-injection and spin-detection efficiencies, η_i and η_d.

plot $\Delta U_{nl}/I$ of the nonannealed sample as a function of U_c in the inset of Fig. 2(a). It changes sign for $U_c>0$, i.e., for spin injection. Such behavior has been related to a transition from minority- to majority-spin injection with increasing U_c.[8,19] In the annealed samples, η_i reverses its sign at $U_c<0$, see Fig. 2(b), and at $U_c>0$ only majority spins are injected. Because of the opposite sign of spin injection close to zero bias, also η_d has opposite signs[8] for the annealed and nonannealed samples. In Fig. 2, we therefore plot $-\Delta U_{nl}$ for the nonannealed sample. Although the dependence of η_i on U_c is not understood in detail, it has been related to the interfacial structure between Fe and GaAs (Refs. 14 and 20) or to a confinement layer in the semiconductor,[21] which will be discussed later.

Figure 3 summarizes $\Delta\rho_{nl}(T)$ for nonannealed and annealed samples. For the nonannealed sample, $\Delta\rho_{nl}$ decays exponentially with increasing T up to 200 K. The decay rate is about 0.018 K^{-1} (black line) for both $U_c=-200$ and 100 mV, and significantly smaller for $U_c=0$ mV. Annealing the sample increases $\Delta\rho_{nl}$ at low T but at the same time also the decay rate of $\Delta\rho_{nl}(T)$ increases to 0.030 K^{-1} (red dashed line). This faster decrease results in a signal that at higher T becomes smaller than that of the nonannealed sample. The data for the annealed sample were obtained at $U_c=0$ but similar behavior is observed for $U_c=100$ mV (not shown). This annealing-induced change in $\Delta\rho_{nl}(T)$ is the central result of this paper and will be discussed in the following.

The magnitude of $\Delta\rho_{nl}$ depends on η_i and η_d, as well as on the transport and spin dynamics in the GaAs channel that reduces the injected spin polarization by a factor S at the detection contact. $S(T)$ is characterized by the diffusion constant D and the spin lifetime τ_s, which are obtained from Hanle measurements at different T, as shown in Fig. 4(a). When the spins in the channel precess about a perpendicular magnetic field B_z, $\Delta\rho_{nl}$ decreases because of the distribution

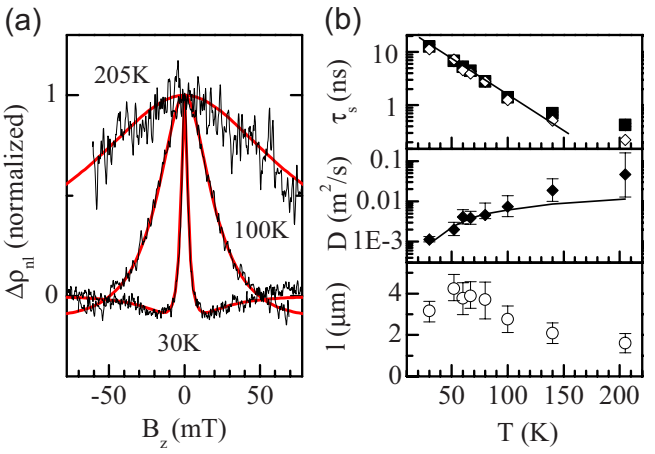

FIG. 4. (Color online) (a) Hanle measurements of $\Delta\rho_{\mathrm{nl}}$ at different temperatures (thin black line) and two-parameter fits (thick red line) on a nonannealed sample. A magnetic field B_z perpendicular to the sample plane was swept at $U_c=-100$ mV, and plotted are the differences between sweeps with antiparallel and parallel magnetization of contacts 2 and 3. (b) Parameters obtained from the Hanle fits. The spin lifetime τ_s is obtained from one- and two-parameter Hanle fits (open diamonds and filled squares), the diffusion constant D from Hanle fits (diamonds) and from Hall measurements (line). The error bars indicate the uncertainty from a background subtraction from the Hanle signal. The spin-diffusion length l is calculated from D and τ_s.

in the arrival times of the injected spins at contact 3. This can be calculated by the one-dimensional Hanle integral[7]

$$\Delta\rho_{\mathrm{nl}} \propto \int_0^\infty \frac{1}{\sqrt{4\pi Dt}} e^{-x^2/4Dt} \cos\left(\frac{g\mu_B B_z t}{\hbar}\right) e^{-t/\tau_s} dt, \qquad (1)$$

where $g=-0.44$ is the electron g factor of GaAs, μ_B the Bohr magneton, $\hbar$ the Planck's constant, and x the distance between injection and detection of the spins. To account for the finite width w_3 of the detection contact, Eq. (1) is integrated for x ranging from a to $a+w_3$. Because of the electric field applied between contacts 1 and 2, it is assumed that all spins are injected at the edge of contact 2 toward contact 3.

Two-parameter fits of the Hanle data with τ_s and D as parameters are shown in Fig. 4(a), and the resulting fit parameters are summarized in Fig. 4(b). The error bar for D arises from an uncertainty in an offset in $\Delta\rho_{\mathrm{nl}}(B_z)$, which becomes larger at higher T, where the tails of the Hanle peak can no longer be measured. For $T>70$ K, the Hanle peak was normalized to the value of $\Delta\rho_{\mathrm{nl}}$ for an in-plane magnetic field sweep. For $T<100$ K, the values of D of the two-parameter Hanle fits match well the data of D obtained from a four-point Hall measurement using the Einstein relation. For $T>100$ K, the Hanle fit values deviate toward higher values, which we attribute to a systematic error that originates in the weak influence of D on the Hanle curves at higher T. We therefore also fit the data with τ_s as the only fit parameter and fix D to the transport value.

In Fig. 4(b), the results for τ_s are shown for both the one- and two-parameter Hanle fits. The two fits yield similar results, namely, a τ_s that decays approximately exponentially with T from 12 ns at 30 K to 200 ps at 205 K. From D and τ_s, the spin-diffusion length $l=\sqrt{D\tau_s}$ is calculated. The combined increase in D and decrease in τ_s lead to only a small decrease in l, from 4 μm at 50 K to 1.6 μm at 200 K. In Ref. 9, $l=2.8$ μm was found at $T=4$ K, whereas Ref. 8 measures $l=6$ μm at 50 K, comparable to our values. It is important to note that postgrowth annealing does not affect the spin transport properties of the GaAs channel and therefore $S(T)$, as verified in separate measurements on an annealed sample.

The contribution S to $\Delta\rho_{\mathrm{nl}}$ can be calculated from Eq. (1) with $B_z=0$. The integration over t yields $S\propto(\tau_s/l)\exp(-x/l)$. S decays exponentially with the separation x between injection and the detection contact, and τ_s/l stems from the integration over time, where spins contribute in a time τ_s and spread over a length l. The proportionality of S to τ_s influences $S(T)$ more strongly than the relatively weak variation in l with T does. $S(T)$ as obtained[22] from the one-parameter Hanle fits is shown in Fig. 3 as triangles, scaled by a factor for better comparison with $\Delta\rho_{\mathrm{nl}}$. The overall T dependence of $\Delta\rho_{\mathrm{nl}}$ is determined from $\eta_i\eta_d S$. Since the decay rate of $\Delta\rho_{\mathrm{nl}}$ of the annealed sample is very similar to that of $S(T)$, $\eta_i\eta_d$ does not change much with T in that sample. However, before annealing, $\Delta\rho_{\mathrm{nl}}$ decreases significantly less, amounting to a factor of 3.7 between 30 and 140 K. This suggests that $\eta_i\eta_d$ increases with T below 140 K. Above 140 K, the slope of $\Delta\rho_{\mathrm{nl}}(T)$ is similar to that of $S(T)$ for both the annealed and the nonannealed samples.

To ensure that Eq. (1) and thus $S(T)$ does not overestimate the decay rate attributed to the GaAs channel, some care has to be taken. In fact, there are several limitations to Eq. (1). First, it is derived in the limit of small spin polarization in the GaAs channel by assuming that there the spin-injection rate does not depend on the spin polarization in the GaAs channel. More generally, the spin-injection rate is proportional to the difference between η_i and the spin polarization in the GaAs channel. This modification is equivalent to adding an effective spin-decay rate $1/\tau_0$, given by the rate of injected electrons divided by the number of electrons in the channel below the injection contact. For our sample geometry, we obtain $\tau_0\approx 10$ ns for a typical current of $I=50$ μA, which is comparable to the spin lifetime of 12 ns at 30 K. The result is that S saturates with increasing τ_s. From a solution of the spin drift-diffusion equation, we find that the corresponding reduction in S is smaller than 30% at 30 K. Second, Eq. (1) neglects the drift of spin polarization toward contact 1. This effect has an influence on S that is smaller than 10% for $I=50$ μA at $U_c=-100$ mV and at 30 K. We can also neglect that dynamic nuclear polarization enhances the applied field[17,23] at small T, which would lead to overestimated values for τ_s. Such dynamic nuclear polarization sensitively depends on a misalignment between sample normal and B_z, and we do not find large variations in the measured τ_s above 30 K. Corrections from the three-dimensional nature of the sample including the finite thickness, inhomogeneous doping of the transport layer, and the finite bar width will also not change the slope of $S(T)$ significantly.

Considering the limitations above, we estimate that the decay rate of S between 30 and 140 K is at least 0.025 K^{-1},

corresponding to a loss of spin polarization in the channel of a factor of at least 16 when T is increased from 30 to 140 K. In this temperature range, however, $\Delta\rho_{\mathrm{nl}}$ measured in the nonannealed sample exhibits a much weaker decrease, namely, only by a factor of 7, whereas for the annealed sample the factor increases to 27. These strong, annealing-induced changes must be related to a modification of the spin-injection or spin-detection efficiency that occurs at the interface. They are concomitant with a shift from minority- to majority-spin injection. We recall that annealing at moderate T is known to affect only the Fe/GaAs(001) interface region, giving rise to structural changes that lead to an enhanced crystal order[15,24] and enhanced polarization injection efficiency.[24,25] The important result is that before moderate postgrowth annealing, $\eta_i \eta_d$ increases with increasing T. Such an increase is likely to be related to a change in the weighting of minority- and majority-spin processes.[26] The spin-filter effect due to symmetry conservation of the coupling between the Fe and GaAs wave functions at the interface strongly favors majority-spin injection[27] for the case of well-ordered Fe/GaAs interfaces. On the other hand, a resonant state arising from interface layers promotes minority-spin injection.[20] In addition, the existence of a bound state in the semiconductor close to the interface can influence both the size and sign of accumulated spin polarization.[21] The exact balance of minority- and majority-spin contributions is determined by the interplay of all these effects.

An essential question is how a change in T can redistribute the weight of the individual contributions. As T is increased, the distribution of electrons that tunnel through the Schottky barrier extends toward higher energies at which the tunneling probability is significantly larger. This change in energy and a simultaneous modification of the in-plane electron momentum of the tunneling electrons may influence the resonance with the minority peak.[20] An additional role could be played by a change in the overlap of GaAs and Fe wave functions that determines the spin filtering efficiency, as well as by a T-dependent variation in the occupation of a semiconductor bound state.

The similar decay rate found for positive and negative U_{c} in the nonannealed sample is an indication that not the spin-injection efficiency η_i is responsible for the positive T dependence at these values of U_{c} but rather the spin-detection efficiency η_d caused by a shift toward the minority peak as T is increased. The bias U_{c} provides a handle to adjust whether the energy of the relevant electrons at the injection contact is above or below the minority peak. Since temperature shifts this energy in one direction only, η_i is expected to increase or decrease with T depending on whether U_{c} is slightly above or below the peak. Within this picture, η_i does not depend on T away from the peak. This explanation is strongly supported by the observation that the zero crossing of $\Delta U_{\mathrm{nl}}(U_{\mathrm{c}})$ shifts toward higher U_{c} when T is increased [inset of Fig. 2(a)]. Because the zero crossing occurs at the crossover from minority- to majority-spin injection, this indicates that around $U_{\mathrm{c}}=0$ temperature shifts the relevant spin injection toward the minority peak. With increasing T, the majority contribution moves farther away from $U_{\mathrm{c}}=0$ and the minority peak gains in strength. This results in a positive T dependence of η_i at $U_{\mathrm{c}}=0$ and by reciprocity also of η_d. Far away from U_c, only the increase in η_d is seen in $\Delta\rho_{\mathrm{nl}}$, whereas at $U_{\mathrm{c}}=0$, both η_i and η_d contribute, leading to an even slower decay of $\Delta\rho_{\mathrm{nl}}$, in agreement with our data, see Fig. 3.

In conclusion, we observe a strong change in the temperature dependence of the nonlocal spin resistance $\Delta\rho_{\mathrm{nl}}$ upon postgrowth sample annealing, which we relate to a change in the T dependence of the spin-transfer efficiency at the injection and detection contacts. For annealed samples, the spin-transfer efficiencies increase with T up to 140 K. Such behavior is likely associated with an interplay of interface-related mechanisms that more and more favors the minority spin as T is increased.

We acknowledge valuable discussions with Rolf Allenspach and technical support from Meinrad Tschudy, Daniele Caimi, Ute Drechsler, and Martin Witzig.

*gsa@zurich.ibm.com

[1] S. F. Alvarado and P. Renaud, Phys. Rev. Lett. **68**, 1387 (1992).
[2] Y. Ohno, D. K. Young, B. Beschoten, F. Matsukura, H. Ohno, and D. D. Awschalom, Nature (London) **402**, 790 (1999).
[3] R. Fiederling, M. Keim, G. Reuscher, W. Ossau, G. Schmidt, A. Waag, and L. W. Molenkamp, Nature (London) **402**, 787 (1999).
[4] H. J. Zhu, M. Ramsteiner, H. Kostial, M. Wassermeier, H.-P. Schönherr, and K. H. Ploog, Phys. Rev. Lett. **87**, 016601 (2001).
[5] A. T. Hanbicki, B. T. Jonker, G. Itskos, G. Kioseoglou, and A. Petrou, Appl. Phys. Lett. **80**, 1240 (2002).
[6] M. Johnson and R. H. Silsbee, Phys. Rev. Lett. **55**, 1790 (1985).
[7] F. J. Jedema, A. T. Filip, and B. J. van Wees, Nature (London) **410**, 345 (2001).
[8] X. Lou, C. Adelmann, S. A. Crooker, E. S. Garlid, J. Zhang, K. S. M. Reddy, S. D. Flexner, C. J. Palmstrøm, and P. A. Crowell, Nat. Phys. **3**, 197 (2007).
[9] M. Ciorga, A. Einwanger, U. Wurstbauer, D. Schuh, W. Wegscheider, and D. Weiss, Phys. Rev. B **79**, 165321 (2009).
[10] O. M. J. van 't Erve, A. T. Hanbicki, M. Holub, C. H. Li, C. Awo-Affouda, P. E. Thompson, and B. T. Jonker, Appl. Phys. Lett. **91**, 212109 (2007).
[11] I. Appelbaum, B. Huang, and D. J. Monsma, Nature (London) **447**, 295 (2007).
[12] N. Tombros, C. Jozsa, M. Popinciuc, H. T. Jonkman, and B. J. van Wees, Nature (London) **448**, 571 (2007).
[13] G. Salis, R. Wang, X. Jiang, R. M. Shelby, S. S. P. Parkin, S. R. Bank, and J. S. Harris, Appl. Phys. Lett. **87**, 262503 (2005).
[14] B. D. Schultz, N. Marom, D. Naveh, X. Lou, C. Adelmann, J. Strand, P. A. Crowell, L. Kronik, and C. J. Palmstrøm, Phys. Rev. B **80**, 201309(R) (2009).
[15] J. M. Shaw and C. M. Falco, J. Appl. Phys. **101**, 033905 (2007).
[16] F. Bianco, P. Bouchon, M. Sousa, G. Salis, and S. Alvarado, J.

Appl. Phys. **104**, 083901 (2008).
[17] G. Salis, A. Fuhrer, and S. F. Alvarado, Phys. Rev. B **80**, 115332 (2009).
[18] P. Zahl, M. Bammerlin, G. Meyer, and R. R. Schlittler, Rev. Sci. Instrum. **76**, 023707 (2005).
[19] J. Moser *et al.*, Appl. Phys. Lett. **89**, 162106 (2006).
[20] A. N. Chantis, K. D. Belashchenko, D. L. Smith, E. Y. Tsymbal, M. van Schilfgaarde, and R. C. Albers, Phys. Rev. Lett. **99**, 196603 (2007).
[21] H. Dery and L. J. Sham, Phys. Rev. Lett. **98**, 046602 (2007).
[22] For calculation of $S(T)$, an additional integration over the width of the detection contact did not change the slope of $S(T)$.
[23] X. Lou, C. Adelmann, M. Furis, S. A. Crooker, C. J. Palmstrøm, and P. A. Crowell, Phys. Rev. Lett. **96**, 176603 (2006).
[24] T. J. Zega, A. T. Hanbicki, S. C. Erwin, I. Žutić, G. Kioseoglou, C. H. Li, B. T. Jonker, and R. M. Stroud, Phys. Rev. Lett. **96**, 196101 (2006).
[25] C. Adelmann, X. Lou, J. Strand, C. J. Palmstrøm, and P. A. Crowell, Phys. Rev. B **71**, 121301(R) (2005).
[26] Irrespective of sample annealing, η_d also depends on the density of states in GaAs at the Fermi energy and thus on carrier density. In the measured T range, we observe only a small increase in the carrier density, from 5 to 6×10^{16} cm^{-3}.
[27] O. Wunnicke, P. Mavropoulos, R. Zeller, P. H. Dederichs, and D. Grundler, Phys. Rev. B **65**, 241306(R) (2002).